LETTERS

Strained silicon as a new electro-optic material

Rune S. Jacobsen[1], Karin N. Andersen[1]†, Peter I. Borel[1], Jacob Fage-Pedersen[1], Lars H. Frandsen[1], Ole Hansen[2], Martin Kristensen[1]†, Andrei V. Lavrinenko[1], Gaid Moulin[1], Haiyan Ou[1], Christophe Peucheret[1], Beáta Zsigri[1] & Anders Bjarklev[1]

For decades, silicon has been the material of choice for mass fabrication of electronics. This is in contrast to photonics, where passive optical components in silicon have only recently been realized[1,2]. The slow progress within silicon optoelectronics, where electronic and optical functionalities can be integrated into monolithic components based on the versatile silicon platform, is due to the limited active optical properties of silicon[3]. Recently, however, a continuous-wave Raman silicon laser was demonstrated[4]; if an effective modulator could also be realized in silicon, data processing and transmission could potentially be performed by all-silicon electronic and optical components. Here we have discovered that a significant linear electro-optic effect is induced in silicon by breaking the crystal symmetry. The symmetry is broken by depositing a straining layer on top of a silicon waveguide, and the induced nonlinear coefficient, $\chi^{(2)} \approx 15\,\mathrm{pm\,V^{-1}}$, makes it possible to realize a silicon electro-optic modulator. The strain-induced linear electro-optic effect may be used to remove a bottleneck[5] in modern computers by replacing the electronic bus with a much faster optical alternative.

The inversion symmetry of a non-strained silicon crystal prohibits the existence of a linear electro-optic effect[3]. However, we have found that the symmetry can be broken by applying an asymmetric strain to the crystal by depositing a straining layer on top of it (Fig. 1), hence creating a linear electro-optic effect in silicon. In other words, when silicon is properly strained, its bulk refractive index (n) varies linearly as a function of external applied electric field (E). In the present structure, we used silicon nitride glass (Si_3N_4) as a straining layer[6]. The amorphous Si_3N_4 layer is compressively strained, that is, it tries to expand the structure underneath in both horizontal directions.

The ability to induce a change in the refractive index can be applied to make an amplitude modulator using a Mach–Zehnder interferometer (Fig. 2), where an applied electric field determines whether or not incident light is transmitted through the modulator. Such an electro-optic modulator[7] is typically used when transmitting data, where transmitted light corresponds to a '1' bit and no light to a '0' bit.

The effect of the material nonlinearity[8] $\chi^{(2)}$ is enhanced if the waveguide possesses a permanently enlarged group index, n_g. It is theoretically predicted[9] that the enhancement scales linearly with the group index. Here, the enhanced nonlinear coefficient $\chi^{(2)}_{enh}$ is therefore defined as:

$$\chi^{(2)}_{enh} \equiv \frac{n_g}{n}\chi^{(2)} \quad (1)$$

An enlarged n_g can for instance be obtained by guiding the light in a photonic crystal waveguide[10] (PCW), which is a waveguide surrounded by a periodically microstructured material[11–13] (Fig. 2). This is the approach that was followed in this work when the strain-induced nonlinearity was discovered. Here, the microstructure consists of silicon with holes that are partially filled with glass and air, giving rise to large material index variations. The period of the structure is on the same scale as the wavelength of the incident light. The result is a waveguide with extremely high group indices—for example, reaching values above 230 for the investigated structure[14].

The group index of a PCW is highly polarization-dependent, and in the present work only transverse electric (TE) light is considered. The experimental method applied to ensure TE polarization of the light transmitted through the PCW is described in detail elsewhere[14]. As the electric modulation field is applied in the x-direction (the

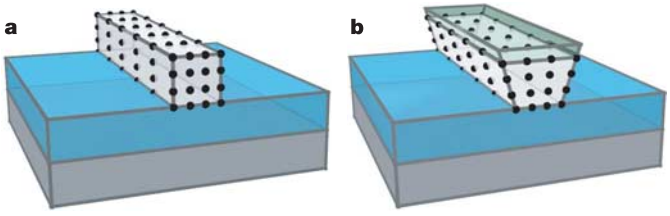

Figure 1 | Applying strain to crystalline silicon. a, Waveguide fabricated in the top layer of an SOI wafer. **b**, The same waveguide with a straining layer deposited on top. The straining layer breaks the inversion symmetry and induces a linear electro-optic effect.

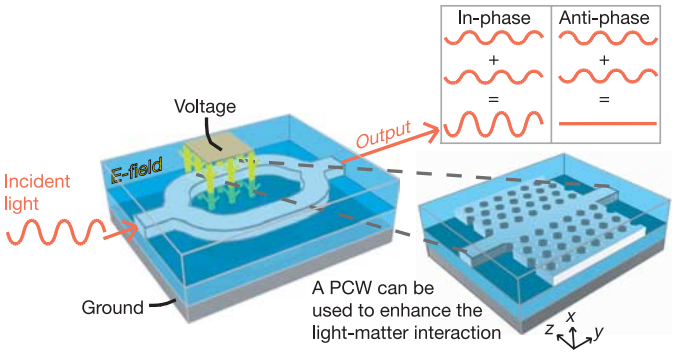

Figure 2 | Diagram of a Mach–Zehnder modulator. Incident light is split into two waveguides. The output amplitude depends on the phase difference at recombination. As shown at top right, in-phase recombination gives a '1' bit output while anti-phase recombination gives a '0' bit output. If the straight waveguide in the Mach–Zehnder modulator is replaced with a PCW as illustrated with the magnified waveguide at bottom right, the effect of a material nonlinearity can be enhanced.

[1]COM•DTU, Department of Communications, Optics & Materials, Building 345V, Nano•DTU, Technical University of Denmark, DK-2800 Kgs. Lyngby, Denmark. [2]CINF, MIC-Department of Micro and Nanotechnology, Building 345E, Nano•DTU, Technical University of Denmark, DK-2800 Kgs. Lyngby, Denmark. †Present addresses: MIC, Building 345E, Technical University of Denmark, DK-2800 Kgs. Lyngby, Denmark (K.A.); iNANO and IFA, University of Aarhus, Ny Munkegade, Building 1520, DK-8000 Århus C, Denmark (M.K.).

coordinate system is shown in Fig. 2) and the light is polarized in the z-direction (TE-polarized), the measured element of the $\chi^{(2)}$ tensor is $\chi^{(2)}_{zzx}$. In the investigated structure, a spacing layer of silica glass (SiO_2) was sandwiched between the silicon waveguide and the straining Si_3N_4 glass (Fig. 3a). By this arrangement, the guided light is confined well below the Si_3N_4 straining layer; that is, the optical field does not extend to this layer. This arrangement ensures that the only influence of the Si_3N_4 layer on the silicon waveguide is a physical strain, exerted through the SiO_2 layer. By measuring $\chi^{(2)}_{enh,zzx}$ both before and after deposition of the Si_3N_4 straining layer, it is demonstrated that the observed linear electro-optic effect is strain-induced.

The measurement before deposition of the straining Si_3N_4 was performed at wavelengths with particularly high n_g values of ~70 and ~180 to ensure optimal detection. A maximum $\chi^{(2)}_{enh,zzx}$ of $\sim 60\,\mathrm{pm\,V^{-1}}$ was found (Fig. 3b) for the highest n_g value at a wavelength of 1,561.468 ± 0.005 nm. The existence of this small but non-zero $\chi^{(2)}_{enh,zzx}$ before deposition of the straining layer is due to a small tensile strain in the upper SiO_2 layer—the SiO_2 spacing layer tries to contract in the horizontal directions. After deposition of the straining Si_3N_4 layer, a $\chi^{(2)}_{enh,zzx}$ of $\sim 830\,\mathrm{pm\,V^{-1}}$ was found at exactly the same wavelength (1,561.468 ± 0.005 nm), so the straining layer increased $\chi^{(2)}_{enh,zzx}$ in the silicon by one order of magnitude (Fig. 3b).

The difference in the induced nonlinear coefficient before and after depositing the Si_3N_4 layer is not only caused by the different magnitudes of strain, but also by the different signs of the strain. The upper SiO_2 layer tries to contract, which is only possible if the whole structure bends like a deep plate. This deformation is only minor, as the thick supporting wafer is extremely difficult to bend. After depositing the Si_3N_4 layer, the sign of the strain is changed, and the top layers now try to expand in the horizontal directions. This expansion can be partially accommodated by a slight wafer bending and partially by introducing strong local deformations near each hole. As a result, the compressive strain is more effective in deforming the waveguiding silicon layer. A Si_3N_4 top layer is of course not required, as strain can also be obtained by altering the deposition conditions of the SiO_2 layer. In fact, another structure was fabricated, in which the SiO_2 layer deposited directly on top of the PCW was grown with a surplus of silicon radicals. Without any additional layers, a $\chi^{(2)}_{enh,zzx}$ nonlinearity was induced. The size of this nonlinearity was about two-thirds of what was obtained when the Si_3N_4 straining layer was used.

By comparing $\chi^{(2)}_{enh,zzx}$ with an independent measurement of the group index (Fig. 4), it is confirmed that the wavelength-dependent changes of $\chi^{(2)}_{enh,zzx}$ are caused by dispersion of the group index. This is, to our knowledge, the first clear experimental verification of the theoretically predicted[9] linear relationship (equation (1)) between group index and enhanced nonlinear coefficient. A previous experiment[15] has shown the existence of an enhancement effect, but it did not verify the predicted linear relationship. To consolidate this result, it can be added that the measured group index was found to be in excellent agreement with both two- and three-dimensional finite-difference time domain (FDTD) calculations performed using the time-of-flight principle. Both the group index measurement and the FDTD calculations are described in detail elsewhere[14].

Several experiments were performed to verify that the observed change in refractive index is due to a genuine $\chi^{(2)}_{zzx}$ rather than being caused by other previously reported effects in silicon[16] (that is, by thermo-optic, photo-elastic, photo-electric or interface effects, or by an effective $\chi^{(2)}_{zzx}$ originating from $\chi^{(3)}_{zzxx}$).

First, to rule out a thermo-optic and/or a photo-elastic effect, it is noted that both effects are independent of the sign of the electric field. Hence, for these effects the response for an applied sinusoidal modulation, $\sin(\omega t)$, is $|\sin(\omega t)|$, which has a large frequency component at 2ω. However, no refractive index change was observed at the frequency 2ω. Second, to show that an effective second-order nonlinearity $\chi^{(2)}_{eff,zzx}$, originating from the combination of $\chi^{(3)}_{zzxx}$ and a frozen-in electric field[17], does not contribute, $\chi^{(2)}_{enh,zzx}$ was measured while applying a large d.c. field ($>40\,\mathrm{V\,\mu m^{-1}}$ over the silicon layer) across the structure. The value of $\chi^{(2)}_{enh,zzx}$ was unaffected by the size and sign of the applied d.c. field, thus excluding a $\chi^{(2)}_{eff,zzx}$ contribution. We note that in the investigated PCW structure, carriers can move in the horizontal direction in the waveguiding layer and thereby move in and out of the silicon region underneath the electrode. The experiment that excluded a $\chi^{(2)}_{eff,zzx}$ contribution also demonstrates that a possible field-induced change in carrier concentration does not play a role, as the large applied positive d.c.

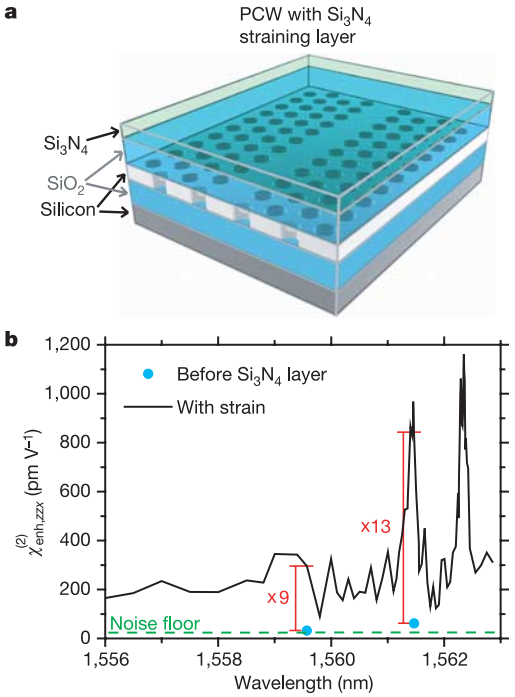

Figure 3 | Effect of straining the silicon structure. **a**, Diagram of the investigated PCW. **b**, Enhanced nonlinearity $\chi^{(2)}_{enh,zzx}$ measured before (blue points) and after (black line) applying the straining layer. A strain-induced increase in $\chi^{(2)}_{enh,zzx}$ by one order of magnitude is observed, compared to the weakly strained structure before deposition of Si_3N_4. The noise floor is shown as the dashed green line.

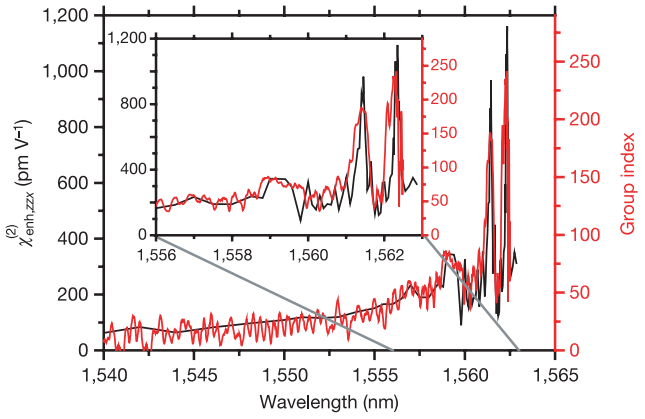

Figure 4 | Experimental verification of the linear enhancement of $\chi^{(2)}_{enh,zzx}$ with the group index. The enhanced nonlinear coefficient $\chi^{(2)}_{enh,zzx}$ (black) of the strained silicon is plotted together with the group index (red) of the photonic crystal waveguide. The inset shows the details in the wavelength range where the fluctuations of the group index are largest.

field efficiently depleted the silicon for carriers and, hence, made carrier transportation impossible.

Third, to investigate if carriers generated by the photo-electric effect contributed to an index change, the experiment with an applied d.c. field was repeated in the dark, ensuring that no photo-generated carriers were present. The photon energy of the incident laser light at ~1,550 nm is lower than the silicon bandgap, that is, the possible carrier contribution from this light is negligible as it only arises from higher-order effects, like two-photon absorption. The result of the measurement was unaffected by the applied d.c. field even when no carriers were generated by light absorption. Hence, the observed refractive index change does not originate from a photo-electric effect.

Fourth, to evaluate the existence of possible effects originating from the interfaces between different materials, a new structure was fabricated. A ~1-μm-wide single-mode rib waveguide was defined in a similar silicon-on-insulator (SOI) wafer with a ~340-nm-thick top silicon layer, by etching only ~30 nm down on both sides of the waveguide core. The fabrication methods applied for deposition of the spacing SiO_2 and the straining Si_3N_4 layers on the PCW were reused to deposit identical layers on top of this shallow etched waveguide. The waveguide fabricated in this way has the same interfaces as the described PCW structure, but the lack of holes in the waveguiding silicon layer hinders local spatial deformation of the silicon crystal. To obtain a large light–matter interaction for such a waveguide, possessing a normal group index ($n_g \approx 3.6$), a 500 times longer (1 cm) waveguide was characterized. No $\chi^{(2)}_{zzx}$ was observed, that is, the $\chi^{(2)}_{zzx}$ value for this structure was below 0.02 pm V^{-1}. This finally substantiates that the observed change in refractive index is caused by a genuine $\chi^{(2)}_{zzx}$ effect originating from deformation of the silicon crystal.

In order to compare the strain-deformed silicon material with other known nonlinear materials, one must distinguish between the enhanced nonlinearity $\chi^{(2)}_{enh}$ and the material nonlinearity $\chi^{(2)}$. The magnitude of $\chi^{(2)}_{enh}$ is governed both by the material's nonlinear coefficient and by the group index (equation (1)), where the group index is determined by the design of the waveguide. To make a fair comparison between different nonlinear materials, one must compare quantities that are independent of the waveguide design, that is, one must compare the material $\chi^{(2)}$ values. The material $\chi^{(2)}_{zzx}$ value is determined to be ~15 pm V^{-1} for the examined strain-deformed silicon from the relationship $\chi^{(2)} = (n/n_g)\chi^{(2)}_{enh}$, by inserting the bulk refractive index of silicon ($n = 3.5$) and the two independent measurement curves for $\chi^{(2)}_{enh,zzx}$ and for n_g (Fig. 4).

It is relevant to compare the size of the strain-induced material nonlinearity in silicon (~15 pm V^{-1}) with that of the commonly applied nonlinear material, $LiNbO_3$. In $LiNbO_3$, the largest $\chi^{(2)}$ tensor component[7] ($\chi^{(2)}_{zzz}$) is ~ 360 pm V^{-1}. However, the required electrode spacing must be considered, as a design aim for a modulator is to reduce the required driving voltage, not the electric field. The large vertical index step in an SOI waveguide (for example, in a photonic wire[18]) allows an ~9 times smaller electrode spacing compared to a $LiNbO_3$ waveguide[19], and hence the difference in required driving voltage is reduced accordingly. Moreover, the material $\chi^{(2)}$ value of strained silicon reported here may increase significantly if the silicon crystal is allowed to deform more freely, using a photonic wire (Fig. 1) instead of a PCW. One of the current advantages of $LiNbO_3$ is the low loss of 0.2 dB cm^{-1} obtainable in a waveguide[20]. Currently the lowest reported optical propagation loss in a silicon photonic wire[21] is 0.8 dB cm^{-1}. However, the loss in a photonic wire is caused by surface roughness[21] and it can be reduced by further process development. The advantage of silicon in comparison with $LiNbO_3$ is the possibility of applying cheap standard fabrication techniques used for fabrication of CMOS circuits. The silicon modulator can also be integrated monolithically with an electronic driver circuit and hybridized with existing semiconductor lasers.

The strain-induced nonlinearity is not the only possibility for realizing an optical modulator in silicon. A modulator based on changing the carrier concentration has been demonstrated[22], and a significant increase of the modulation speed up to 10 Gbit s^{-1} has recently been obtained[23,24]. However, changing the carrier concentration requires a large a.c. current[24] of ~0.2 A (r.m.s.) through the silicon structure. In contrast, in the strained silicon presented here, there is no current through the waveguide structure. Moreover, the speed of the strained silicon modulator is not limited by charge mobility or charge recombination times. Thus, the discovered linear electro-optic effect may provide a decisive step towards utilization of active silicon-based photonics.

METHODS

Sample fabrication. A 20-μm-long straight W1 PCW was fabricated[25] using CMOS technology to etch holes with a diameter of 255 ± 5 nm placed in a triangular pattern with pitch $\Lambda = 435$ nm in the top layer of a SOI wafer. The waveguide was defined in the ΓK direction by removing one row of holes. The SOI wafer consisted of 220 ± 20 nm single crystalline silicon on 1,000 ± 22.5 nm SiO_2, placed on a single crystalline silicon wafer. The silicon was doped with boron, and the resistivity of the top and bottom <100> oriented silicon layers are 8.5–11.5 and 14–18.9 Ω cm, respectively. The cut-off wavelength of the generic PCW was located at 1,625 nm. The structure was then oxidized in a dry O_2 atmosphere at 1,050 °C for 20 min to increase the effective diameter of the holes in the silicon to 282 ± 5 nm, and simultaneously the thickness of the top silicon layer was reduced to 200 ± 20 nm. The oxidation produced glass rings with a thickness of ~40 nm on the inner side of the silicon holes, and the cut-off wavelength moved down to 1,552.5 nm. A SiO_2 spacing layer with a thickness of ~1.2 μm partially filling the air holes inside the glass rings was deposited as top cladding, using a standard PECVD technique. The structure was then annealed at 1,050 °C in a dry N_2 atmosphere for 4 h. By also depositing SiO_2 on a blank test wafer, the stress of the spacing layer was measured to be ~0.3 GPa tensile. The deposition of SiO_2 lowered the vertical index step of the PCW to the difference between silicon ($n = 3.476$) and glass ($n = 1.445$), hence moving the cut-off wavelength up to its final value at 1,562.5 nm. After measuring the nonlinearity $\chi^{(2)}_{enh,zzx}$ without the straining layer, a ~0.75-μm-thick Si_3N_4 straining layer was deposited on the same structure using an appropriate PECVD recipe[26]. By depositing Si_3N_4 on a test wafer with ~1 μm thermal oxide on top, the stress was measured to be ~1 GPa compressive. Finally, the nonlinearity $\chi^{(2)}_{enh,zzx}$ was measured again.

Measurement of $\chi^{(2)}_{enh}$. A fibre-based Mach–Zehnder interferometer was used to measure the $\chi^{(2)}_{enh,zzx}$ value. The PCW was placed in one arm of the Mach–Zehnder interferometer and a reference $LiNbO_3$ phase modulator was placed in the other arm. An equipment-limited (~110 V r.m.s. at 200 kHz) a.c. voltage was applied across the PCW, and the induced phase oscillation was then balanced with an identical phase oscillation from the $LiNbO_3$ modulator. When the modulations were balanced, that is, they had equal amplitudes, the output of the Mach–Zehnder interferometer was unaffected by the modulators. The phase oscillation and, hence, $\chi^{(2)}_{enh,zzx}$ for the silicon PCW was then determined by measuring the a.c. voltage applied to the reference $LiNbO_3$ modulator.

Received 4 October 2005; accepted 2 March 2006.

1. Trinh, P. D., Yegnanarayanan, S., Coppinger, F. & Jalali, B. Silicon-on-insulator (SOI) phased-array wavelength multi/demultiplexer with extremely low-polarization sensitivity. *IEEE Photon. Technol. Lett.* **9,** 940–942 (1997).
2. Pavesi, L. & Lockwood, D. J. *Silicon Photonics* (Springer, Berlin, 2004).
3. Reed, G. T. & Png, C. E. J. Silicon optical modulators. *Mater. Today* **8,** 40–50 (2005).
4. Rong, H. *et al.* A continuous-wave Raman silicon laser. *Nature* **433,** 725–727 (2005).
5. Gibbs, W. W. A split at the core. *Sci. Am.* **291,** 96–100 (2004).
6. Madou, M. J. *Fundamentals of Microfabrication* 299–301 (CRC Press, Boca Raton, Florida, 2002).
7. Li, G. L. & Yu, P. K. L. Optical intensity modulators for digital and analog applications. *J. Lightwave Technol.* **21,** 2010–2030 (2003).
8. Butcher, P. N. & Cotter, D. *The Elements of Nonlinear Optics* 5 (Cambridge Univ. Press, Cambridge, UK, 1990).
9. Soljacic, M. & Joannopoulos, J. D. Enhancement of nonlinear effects using photonic crystals. *Nature Mater.* **3,** 211–219 (2004).
10. Notomi, M. *et al.* Extremely large group-velocity dispersion of line-defect waveguides in photonic crystal slabs. *Phys. Rev. Lett.* **87,** 253902 (2001).
11. Joannopoulos, J. D., Villeneuve, P. R. & Fan, S. Photonic crystals: putting a new twist on light. *Nature* **386,** 143–149 (1997).

12. Krauss, T. F., De La Rue, R. M. & Brand, S. Two-dimensional photonic-bandgap structures operating at near-infrared wavelengths. *Nature* **383,** 699–702 (1996).
13. Joannopoulos, J. D., Meade, R. D. & Winn, J. N. *Photonic Crystals: Molding the Flow of Light* (Princeton Univ. Press, Princeton, 1995).
14. Jacobsen, R. S. *et al.* Direct experimental and numerical determination of extremely high group indices in photonic crystal waveguides. *Opt. Express* **13,** 7861–7871 (2005).
15. Hitoshi, N. *et al.* Ultra-fast photonic crystal/quantum dot all-optical switch for future photonic networks. *Opt. Express* **12,** 6606–6614 (2004).
16. Soref, R. A. Silicon-based optoelectronics. *Proc. IEEE* **81,** 1687–1706 (1993).
17. Myers, R. A., Mukherhee, N. & Brueck, S. R. J. Large second-order nonlinearity in poled fused silica. *Opt. Lett.* **16,** 1732–1734 (1991).
18. Vlasov, Y. A. & McNab, S. J. Losses in single-mode silicon-on-insulator strip waveguides and bends. *Opt. Express* **12,** 1622–1631 (2004).
19. Kondo, J. *et al.* 40-Gb/s X-cut $LiNbO_3$ optical modulator with two-step back-slot structure. *J. Lightwave Technol.* **20,** 2110–2114 (2002).
20. Liao, W. J. *et al.* Proton-exchanged optical waveguides fabricated by glutaric acid. *Opt. Laser Technol.* **36,** 603–606 (2004).
21. Lee, K. K., Lim, D. R., Kimerling, L. C., Shin, J. & Cerrina, F. Fabrication of ultralow-loss Si/SiO_2 waveguides by roughness reduction. *Opt. Lett.* **26,** 1888–1890 (2001).
22. Soref, R. A. & Bennett, B. R. Electrooptical effects in silicon. *IEEE J. Quant. Electron.* **QE-23,** 123–129 (1987).
23. Liu, A. *et al.* A high-speed silicon optical modulator based on a metal-oxide-semiconductor capacitor. *Nature* **427,** 615–618 (2004).
24. Liao, L. *et al.* High speed silicon Mach-Zehnder modulator. *Opt. Express* **13,** 3129–3135 (2005).
25. Bogaerts, W. *et al.* Nanophotonic waveguides in silicon-on-insulator fabricated with CMOS technology. *J. Lightwave Technol.* **23,** 401–412 (2005).
26. Rasmussen, F. E. *Electrical Interconnections through CMOS Wafers*. PhD. thesis, Tech. Univ. Denmark (2003); ⟨http://www.mic.dtu.dk/upload/institutter/mic/forskning/mems/report-31102003.pdf⟩.

Acknowledgements We thank R. Kjær and M. Svalgaard for their contributions. This work was supported in part by the NKT academy, the Danish Research Council for Technology and Production Sciences via the PIPE project, by NEDO via the Industrial Technology Research Area and by CINF via the Danish National Research Foundation. All generic SOI PCWs were fabricated within the framework of the European IST project PICCO and in this connection we especially thank W. Bogaerts and R. Baets.

Author Information Reprints and permissions information is available at npg.nature.com/reprintsandpermissions. The authors declare no competing financial interests. Correspondence and requests for materials should be addressed to R.S.J. (Rune@com.dtu.dk).